De novo Metallonucleases Based on Helix–Loop–Helix Motifs

Paola Rossi,[a] Paolo Tecilla,[c] Lars Baltzer,*[b] and Paolo Scrimin*[a]

Abstract: Three new 42-mer peptides (PR I–III) designed to fold into a hairpin helix–loop–helix motif have been prepared. In the peptide sequence two (PR II–III) or four (PR I) copies of an unnatural amino acid bearing a triazacyclononane metal-ion binding site (ATANP) have been inserted in appropriate positions to allow the ligand subunits to face each other either within the same helix or between the two helices of the hairpin motif. Circular dichroism (CD) studies in solution have shown that the apopeptides adopt a well-defined helix–loop–helix tertiary structure that dimerizes in solution at concentrations above 200 μM to form a four-helix bundle. However, the helical content is strongly dependent on pH and metal-ion binding. Both protonation of the amines of the triazacyclononane units present in the ATANP lateral arm and complexation with Zn^{II} ions cause a significant decrease of the helical content of the sequences. The Zn^{II} complexes of the three peptides catalyze the transesterification of the RNA model substrate 2-hydroxypropyl-*p*-nitrophenyl phosphate (HPNP) with different efficiency. The best catalyst appears to be PR I–4 Zn^{II}, that is, the peptide incorporating four ATANP units. Michaelis–Menten saturation kinetics allowed us to estimate that substrate fully bound to the catalyst reacts 380 times faster than in its absence. The kinetic evidence suggests cooperativity between (at least two) metal ions: one activating the nucleophilic species (directly or indirectly) and the other facilitating nucleophilic attack by coordination of the phosphate.

Keywords: enzyme models · kinetics · peptides · phosphate cleavage · zinc

Introduction

The design of synthetic catalysts or molecular devices based on peptide[1] foldamers[2] is an appealing goal for many reasons, for example, the flexibility in the selection of the building blocks, the chirality of the structure, and the possibility to mimic natural systems. If one focuses on hydrolysis catalysts, the most challenging substrates are phosphate esters. Indeed their hydrolysis is so slow under physiological conditions that the most recent estimates place the half-life for the cleavage of dimethyl phosphate in 10^{10} years.[3] Not far from this sluggish reactivity should be that required for hydrolytically cleaving the P–O bond of DNA. RNA is more labile, because the nucleophilic attack on the phosphorus atom is performed intramolecularly by the -O(H) group in the 2′-position of the ribose. Thus, the half-life is, in this case, of only 10^4 years. Nevertheless nature has developed very efficient enzymes that contain and require a multinuclear metal-ion site for activity.[4] These include enzymes able to cleave RNA and DNA.[5] Suitably designed, simple multinuclear metal complexes quite effective in the cleavage of model esters have previously been reported.[6] In some cases these complexes promoted effective cleavage of RNA[7] and, to a lesser extent, of DNA.[8]. These biopolymers are appealing targets, because their selective hydrolysis could have implications for applications such as cancer therapy and gene manipulation.

We have recently reported[9] that the peptide 3_{10}-helix conformation can be used as a robust scaffold[10] to develop effective artificial metallonucleases. This has been achieved by inserting two copies of an amino acid (ATANP[11]) bearing a metal-ion binding site,[9a–c] into proper positions in a short peptide sequence, or by connecting several copies of a short

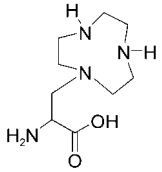

ATANP

[a] Dr. P. Rossi, Prof. P. Scrimin
University of Padova
Department of Chemical Sciences and ITM-CNR Padova Section
Via Marzolo, 1, 35131 Padova (Italy)
Fax: (+39) 049-827-5239
E-mail: paolo.scrimin@unipd.it

[b] Prof. L. Baltzer
Department of Chemistry
Linköping University, 581 83 Linköping (Sweden)
Fax: (+46) 1312-2587
E-mail: Lars.Baltzer@ifm.liu.se

[c] Prof. P. Tecilla
Dipartimento di Scienze Chimiche
Università di Trieste
Via Giorgieri 1, 34127 Trieste (Italy)

 DOI: 10.1002/chem.200400160

sequence also functionalized with such an amino acid to a proper templating unit.[9d]

As an alternative approach to robust, catalytically active foldamers, researchers have focused on longer peptides,[12] of less than 100 residues, with significant results obtained by using the four-helix bundle,[13,14,15] coiled coil,[16] and $\beta\beta\alpha$[17] motifs. Recent studies by one of the laboratories[18] contributing to this paper have clearly shown that the helix–loop–helix motif can be used as a scaffold for the design of new esterolytic catalysts based on $HisH^+$–His cooperative sites.[19] The above catalysts were based on sequences composed of natural amino acids.

We now report our results on the design, synthesis, conformational and kinetic studies of new sequences comprising two or more copies of the unnatural amino acid ATANP resulting in helix–loop–helix forming foldamers. These systems were tested, as their Zn^{II} complexes, as catalysts of the intramolecular transphosphorylation of 2-hydroxypropyl-*p*-nitrophenyl phosphate (HPNP), a model for an RNA phosphate.

Results and Discussion

Peptide design and synthesis: The design of the three peptides PR I–III was based on the sequence of peptides SA-42[19a] and KO-42,[18] which are known to fold into a hairpin helix–loop–helix motif that dimerizes in an antiparallel mode to form a four-helix bundle.[20] In order to maintain the same conformation for the three new peptides, the amino acid sequences of PR I–III were identical to that of KO-42, but for the six His amino acids in positions 11, 15, 19, 26, 30, and 34.

Ac-N-A-A-D-Nle-E-A-A-I-K-**ATANP**(11)-L-A-E-**ATANP**(15)-Nle-A-A-K-
-G-P-V-D-
H_2N-G-A-R-A-F-A-E-F-**ATANP**(34)-K-A-L-**ATANP**(30)-E-A-Nle-Q-A-A-

PRI

Ac-N-A-A-D-Nle-E-A-A-I-K-A(11)-L-A-E-R(15)-Nle-A-A-K-
-G-P-V-D-
H_2N-G-A-R-A-F-A-E-F-**ATANP**(34)-K-A-L-**ATANP**(30)-E-A-Nle-Q-A-A-

PRII

Ac-N-A-A-D-Nle-E-A-A-I-K-A(11)-L-A-E-**ATANP**(15)-Nle-A-A-K-
-G-P-V-D-
H_2N-G-A-R-A-F-A-E-F-R-(34)-K-A-L-**ATANP**(30)-E-A-Nle-Q-A-A-

PRIII

The artificial amino acid ATANP was inserted in positions 11, 15, 30, and 34 in PR I, 30 and 34 in PR II, and 15 and 30 in PR III. Assuming an α-helix conformation, the insertion of ATANP in positions i, $(i+4)$ allows the lateral arms, bearing the ligand subunit, to face each other in the same helix. In contrast, when they are on two different helices the close interaction is guaranteed by the hairpin conformation adopted by these peptides (see below). In all three systems the His residues were replaced by Lys and Glu residues in positions 19 and 26, respectively. This substitution is known, from previous studies on the parent peptide SA-42,[19a] to preserve the helical conformation. The choice of the amino acids replacing the other two His residues in PR II and PR III was based on their propensity for helical structure formation. Because of this, when fully folded the three peptides should assume a helix–loop–helix conformations; that for PR I is shown in Figure 1. The conformational aspects will be discussed in more detail in the section below.

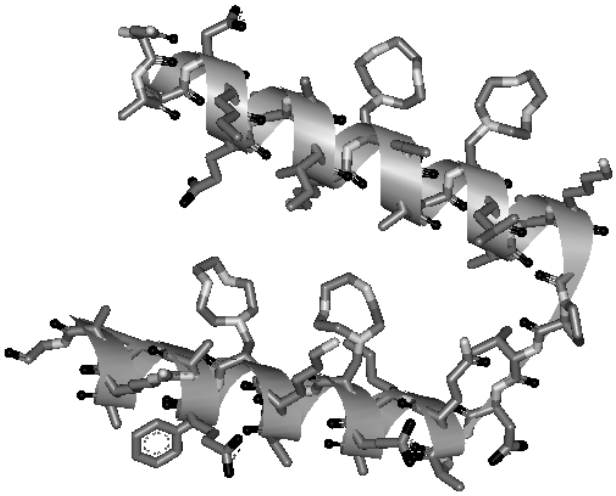

Figure 1. Helix–loop–helix conformation likely adopted by peptide PR I in its folded state.

The syntheses were performed by means of standard solid-phase procedures on an automated peptide synthesizer following an Fmoc protocol. The introduction of the artificial amino acid ATANP into the sequence did not present any problem in spite of the bulkiness of the Boc-protected azacrown present in its lateral arm. Accordingly, the three peptides were obtained in good yields and could be purified easily by reverse-phase HPLC. Synthetic details and identification of the peptides are reported in the Experimental Section.

Solution structure: As mentioned above the sequences of PR I–III were chosen based on those of two parent peptides, SA-42 and KO-42, whose helix–loop–helix conformations were unambiguously assigned by NMR and CD spectroscopy and by equilibrium sedimentation ultracentrifugation.[18,19a] The reported mean residue ellipticities at 222 nm are -25000 ± 1000 deg cm^2 dmol^{-1} and -24000 ± 1000 deg cm^2 dmol^{-1} for SA-42 and KO-42, respectively, and correspond to a helical content of approximately 60–70%.[21,22] The CD spectra of PR I–III are typical of helical polypeptides (Figure 2) with minima at 208 and 222 nm. The mean residue ellipticities at 222 nm are -25000 ± 1000 deg cm^2 dmol^{-1} for PR II and PR III, respectively, and -18000 ± 1000 deg cm^2 dmol^{-1} for PR I at 298 K in pH 7 aqueous solution. The measured ellipticities allow one to estimate a helical content of 70% for PR II and PR III, and of 50% for PR I.[21,22] The CD spectra are strongly dependent on pH, as shown in the pH profiles of Figure 3. All three peptides showed a significant increase in the absolute value of the

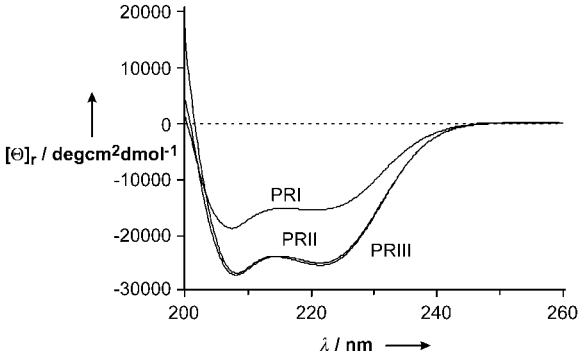

Figure 2. CD spectra of peptides PR I–III at pH 7, 298 K, [peptide] = 2×10^{-4} M.

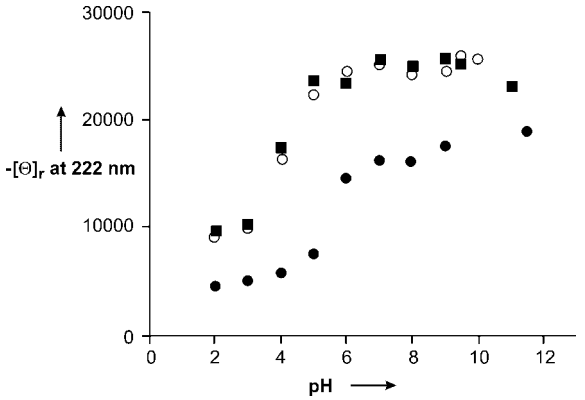

Figure 3. Mean residue ellipticity $[\theta]_r$ at 222 nm versus pH for peptide PR I (●), PR II (■), and PR III (○). Conditions: 298 K, [PR I–III] = 0.2 mM.

molar ellipticity upon increasing the pH from 2 to 7. Above this pH they leveled off to their maximum value. The profiles of Figure 3 suggest that the progressive increase of the helical content of each peptide is associated with the deprotonation of the amine groups of the azacrown present in the side chain of the ATANP residues (the reported pK_a for 1,4,7-triazacyclononane are respectively:[23] pK_1 2–3, pK_2 6.84, pK_3 10.44). Thus the electrostatic repulsion between the protonated amines causes a significant disruption of the helical conformation regardless of whether the azacrown moieties are on the same or on different helices. Furthermore, since the ellipticity reaches a plateau region at pH higher than 7 for all peptides, and this value is very similar to that of their parent compounds, it suggests that the presence of a single positive charge per azacrown is not detrimental to the helical conformation. However, with PR I the presence of four ATANP residues in the sequence appears to present a hindrance to the attainment of a fully folded conformation. We speculate that this may be due to the increase of the hydrophilicity of the two helices. Indeed, their close, hydrophobically driven interaction plays a major role in the folding of these sequences.[24] This is also highlighted by the plot in Figure 4 in which the ellipticity versus concentration profiles for the three systems at pH 7 and 298 K are reported.

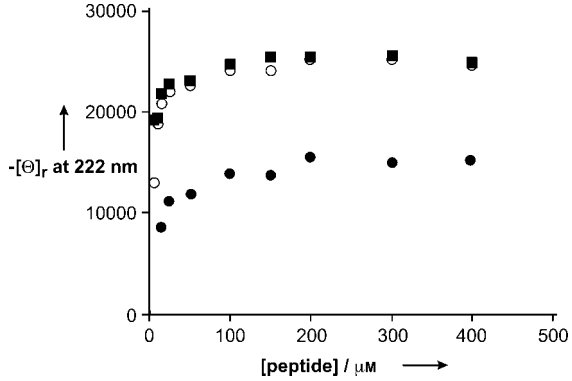

Figure 4. Mean residue ellipticity $[\theta]_r$ at 222 nm as a function of the peptide concentration at 298 K and pH 7 PR I (●), PR II (■), and PR III (○).

The helical content increases up to a concentration ~200 μM for all peptides. In analogy with what is observed with the parent compounds SA-42 and KO-42, this is likely to be associated with their dimerization. In a monomer–dimer equilibrium the absolute value of $[\theta]_{222}$ should increase as a function of the concentration of peptide up to a maximum value, at which the dimer is the predominant species. Thus at concentrations higher than 200 μM, the dimer is likely to be the predominant species with a mean residue ellipticity of -25000 ± 1000 deg cm^2 dmol^{-1} for PR II and PR III, and -18000 ± 1000 deg cm^2 dmol^{-1} for PR I.

The temperature-dependent denaturation process of the peptides was also followed by CD as may be seen for PR III in Figure 5. At 293 K and at the concentration used for the

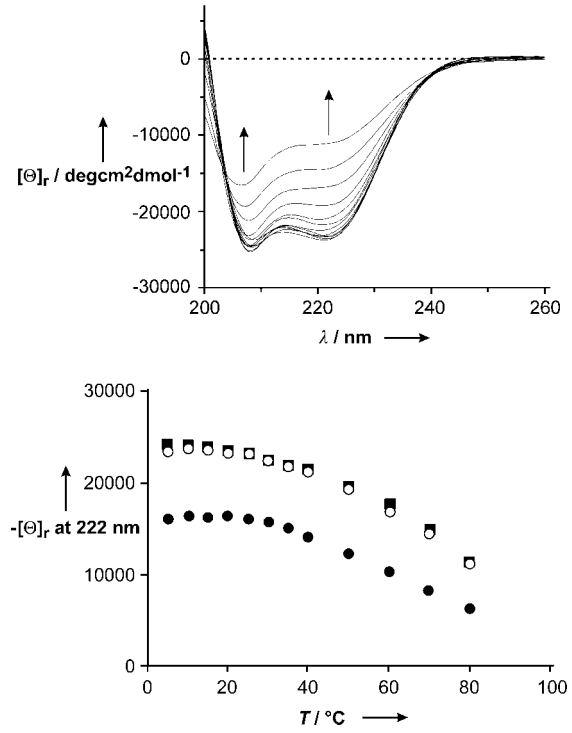

Figure 5. a) CD spectra of PR III (0.2 mM) as a function of increasing temperature. b) Temperature dependence of the mean residue ellipticity $[\theta]_r$ at 222 nm in the case of PR I (●), PR II (■), and PR III (○). Conditions: [peptide] = 0.2 mM, pH 7.

experiments (200 μM, that is, in the presence of the dimer) the molar ellipticity was $-24\,500\ \mathrm{deg\,cm^2\,dmol^{-1}}$ and at 353 K, the maximum temperature explored, it was half this value. Analogous behavior was observed with PR I and PR II (data not shown). The loss of helicity becomes relevant above 313 K. An isodichroic point can be observed at 203 nm (Figure 5a) suggesting a two-state equilibrium between the unfolded (random coil) and folded states.[25] However, the shift from the helical to the random coil conformation does not appear to be highly cooperative (no sharp melting temperature was observed) in line with the molten globule nature[26] of these peptides (and also parents SA-42 and KO-42). Because the CD investigation carried out for PR I–III provides results very similar to those of the parent peptides SA-42 and KO-42, we assume with confidence that they adopt similar conformations (a helix–loop–helix system dimerizing to a four-helix bundle). It is important to point out that at 313 K, which is the temperature used in the following kinetic studies, there is only a loss in helical content of about 10%.

Metal-ion binding: A relevant aspect of our investigation was the study of the ability of our peptides to bind transition-metal ions and the effect of the complex formation on their conformation. Our aim was the synthesis of metal-ion-based catalysts as artificial metallonucleases. Zn^{II} (and Mg^{II}) are the most frequently encountered metal ions in natural nucleases.[4] For this reason in our kinetic experiments we tested our putative catalysts as Zn^{II} complexes. However, for the purpose of addressing the stoichiometry of the binding of transition-metal ions to peptides PR I–III, it was more convenient to follow the complexation of Cu^{II}, since this can be done by UV-visible spectroscopy. The complexes of 1,4,7-triazacyclononane with Cu^{II} show an absorption band with maximum at about 600 nm. Figure 6 reports the titration curves obtained for the three peptides with $Cu(NO_3)_2$ at pH 7 in water ([PR I–III] = 0.2 mM). PR II and PR III can bind up to two equivalents of Cu^{II} ions, and the coordination of the first does not seem to interfere with the coordination of the second. This statement is supported by the monotonic increase of absorbance at 600 nm when up to two equivalents of metal ion are added, that is, the complete saturation with the metal of the two macrocycles. A smaller binding constant for the introduction of the second metal ion, or a change in the coordination sphere with a change of the maximum of absorbance, would have resulted in a change in slope after the addition of the first equivalent. This is indeed the case for PR I; after the addition of three equivalents of Cu^{II} a change in slope can be clearly appreciated, indicating that the complexation of the fourth ion is harder to achieve. Accordingly, complete saturation of the four binding sites in this polypeptide is only observed when at least five equivalents of Cu^{II} are added. The order of binding of the different ATANP in the sequence cannot be determined from the spectroscopic data. In particular we do not know if there is a specific binding site that is particularly reluctant to take up the last metal ion. We may only speculate that ATANP Cu^{II} binding sites in positions 15 or 34 in the sequence, which face two bound Cu^{II} ions on the opposite helix, are those more affected in terms of binding strength.

Complexes of Zn^{II} do not show a similar absorption band in the UV-visible spectrum amenable to a similar binding investigation. We assume that the stoichiometry of binding of this metal ion is not much different from that of Cu^{II}. Its binding strength is, however, 2–4 orders of magnitude lower.[23] Accordingly, the complete saturation of the ligand subunits of PR I should be even more difficult with Zn^{II}. An indirect appreciation of the binding of Zn^{II} to these peptides could be obtained from the effect of the addition of the metal ion on the CD spectra carried out with the aim of evaluating the influence of the metal on the secondary structure. Upon addition of increasing amounts of Zn^{II} to solutions of the three peptides, the absolute value of the mean residue ellipticity at 222 nm tends to decrease up to a complete saturation of the binding sites (Figure 7).[27] This indicates that the complexation of the metal ions has a destabilizing effect on the secondary structure. Lau et al.[28] have reported, for coiled-coil structures, that metal-ion binding induces a shift from the dimer to the monomer thus decreasing the helical content of the polypeptides (see also Figure 4 and previous discussion). It might be that this is the case for our peptides too. Whatever the reason, it is clear that the Zn^{II}-bound peptides are less structured than the corresponding apo systems.

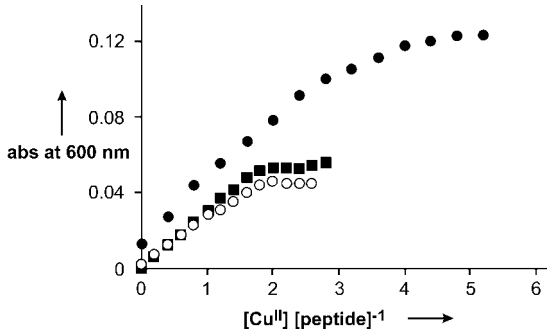

Figure 6. UV-visible titration at 600 nm of PR I (●), PR II (■), and PR III (○) with Cu^{II}. Conditions: [PR I–III] = 0.2 mM, HEPES 50 mM, pH 7.

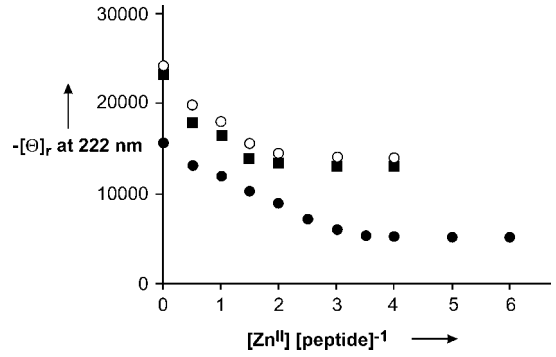

Figure 7. Dependence of the mean residue ellipticity $[\theta]_r$ at 222 nm as a function of the $[Zn^{II}]$/[peptide] ratio for PR I (●), PR II (■), and PR III (○). Conditions: 298 K, pH 7, [PR I-III] = 2×10^{-4} M.

Cleavage studies: The catalytic activities of peptides PR I–III were tested, as Zn^{II} complexes prepared in situ, toward the transesterification reaction of the RNA model substrate HPNP (see Scheme 1). The reactions were carried out with

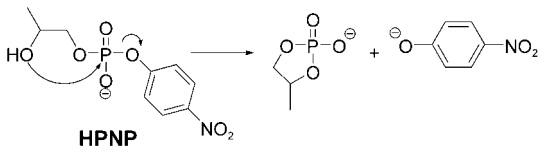

Scheme 1. Transesterification reaction of HPNP.

a tenfold excess of substrate over catalyst, that is, under turnover conditions, at pH 7.4 and 313 K. This temperature causes only a minimum decrease of the helical content of the peptides (see Figure 5b). However, upon formation of the complexes with Zn^{II}, the loss of helical content was significant, particularly for PR I (see Figure 7).

The kinetic plots showed a well-behaved first-order profile, indicating that our systems are real catalysts and no intermediates accumulate during the cleavage process. Table 1

Table 1. Observed second-order rate constants (k_2) for the cleavage of HPNP by Zn^{II} complexes of peptides PR I–III at pH 7.4 (50 mM HEPES, 313 K).

Entry	Catalyst	k_2 [$M^{-1}s^{-1}$]
1	PR I–4 Zn	0.16
2	PR II–2 Zn	0.094
3	PR III–2 Zn	0.084
4	TACN–Zn	0.024
5	3_{10}–2 Zn[a]	0.05

[a] Dinuclear Zn^{II} complex of 3_{10}-helical peptide described in reference [9b].

lists the apparent second-order rate constants (k_2, $M^{-1}s^{-1}$) obtained for the different Zn^{II}–peptide complexes.[29] In spite of the fact that under the conditions used for the kinetic experiments (in the presence of four equivalents of Zn^{II}) PR I was not fully saturated with the metal ions (see discussion in the previous section), it was the best catalyst among the different peptides. Hence a more thorough investigation was carried out with this system.

We examined the catalytic efficiency of PR I by progressively adding Zn^{II} ions to a 2×10^{-5} M solution of the peptide to determine the most catalytically active complex. The initial rates of the HPNP cleavage reaction (v_i, Ms^{-1}) are reported in Figure 8. By analyzing the profile of this curve we learn the following:

1) The apopeptide is modestly active (less than three times faster than the uncatalyzed process).[30] This is in line with results reported by others on the activity in the cleavage of HPNP and RNA by amines/ammonium ions, including triazacyclononane.[31]
2) The most active system is the one fully loaded with Zn^{II} ions. For the saturation of all four ligand subunits an excess of Zn^{II} was required in accord with the Cu^{II} complexation results reported in a previous section.
3) There is cooperativity between the metal centers. Indeed the profile of the curve is sigmoidal indicating a nonlinear increase of activity upon progressive complexation of Zn^{II} ions.

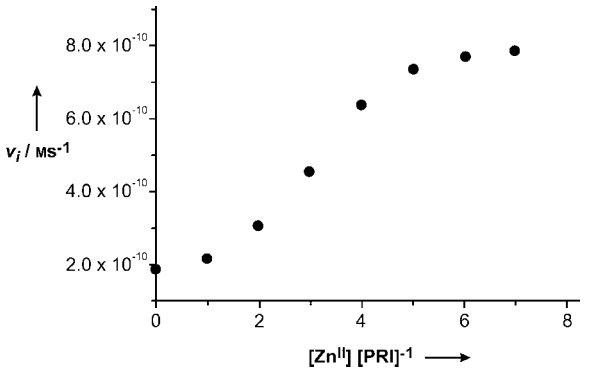

Figure 8. Initial rate of cleavage of HPNP (v_i, Ms^{-1}) as a function of the $[Zn^{II}]/[PR I]$ ratio. Conditions: $[PR I]=2\times10^{-5}$ M, $[HPNP]=2\times10^{-4}$ M, 313 K, pH 7.4, HEPES buffer 50 mM.

One may argue that, since metal ion complexation causes a substantial loss of helicity of the peptide, probably related to the decrease of the amount of dimeric peptide present, the increase of activity could be due to the higher activity of the random coil (monomeric) conformation with respect to the helical one. We cannot rule out that this is the case. However it appears unlikely that a random aggregate of metal centers is more active than an ordered system with the four metal complexes residing on the same side of the helix–loop–helix motif and in close proximity to one another. If, as we consider more likely, the folded peptide is the active species, we underestimate its activity because of the coexistence of the less active, random coil conformation under the conditions of our experiments. It is also conceivable that the catalytic site in the dimeric system is less accessible to the substrate than in the monomeric one.

One important point pertaining to the mechanism of the cleavage process is the binding of the substrate to the catalyst. In the natural enzymes a precise binding of the substrate is necessary to perform the catalytic process. For this reason we performed kinetic measurements at increasing concentration of HPNP and found a Michaelis–Menten behavior indicating that this substrate binds to PR I-4 Zn^{II} (Figure 9). Analysis of the curve indicates a 380-fold rate acceleration over the uncatalyzed cleavage process.[30]

Support to cooperativity between the metal ions was also obtained from the rate vs. pH profile (Figure 10). In this figure we observe that the initial rate value increases with pH up to pH 8, then decreases to reach a minimum at pH 8.5 and increases again. We previously reported[9a,c] that, in the cleavage of HPNP, the kinetically relevant nucleophile bound to a Zn^{II}–triazacyclononane complex has a pK_a in the range 7.7–7.9, very close to the pH at which is observed the maximum in the graph of Figure 9. There are at least two possible explanations for such a behavior. The first

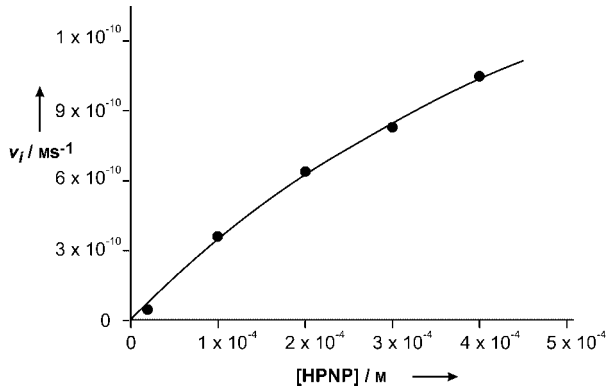

Figure 9. Initial rate of cleavage of HPNP as a function of HPNP concentration in the presence of $2x10^{-5}$ M PRI–4Zn^{II} at pH 7.4 (HEPES 50 mM) and 313 K. The curve is the fitting with the Michaelis–Menten equation.

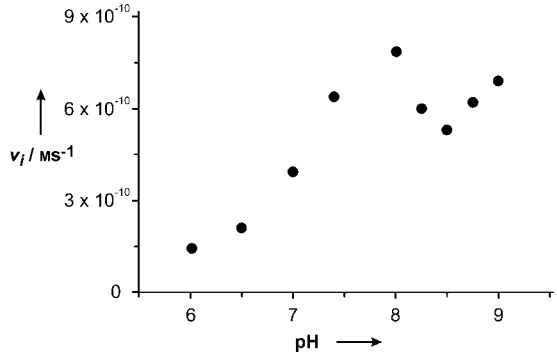

Figure 10. Initial rate versus pH profile for the cleavage of 2×10^{-4} M HPNP by 2×10^{-5} M PRI–4Zn at 313 K. Buffers (50 mM): pH 6.0 and 6.5, MES; pH 7.0–7.5, HEPES; pH 8.0–9.25, CHES.

is that catalysis is due to deprotonation of the substrate hydroxyl, or through direct coordination to a Zn^{II} ion (Figure 11b,d), or indirectly by means of a Zn^{II}-bound water molecule that acts as a general base (Figure 11a,c). A second metal-bound water molecule would act as a general acid to favor the departure of the leaving group (Figure 11a).[32] Alternatively, the second Zn^{II} ion could bind to the P(=O)O-group of the substrate thus activating the attack by the nucleophilic species (Figure 11c). In this last case the decrease in rate would be the result of a decreased binding of the substrate due to the difficulty in displacing a Zn^{II}-bound hydroxyl instead of a water molecule.[33] Our data do not allow us to differentiate between these two mechanisms. Nevertheless both point to a cooperative role of (at least) two metal ions.

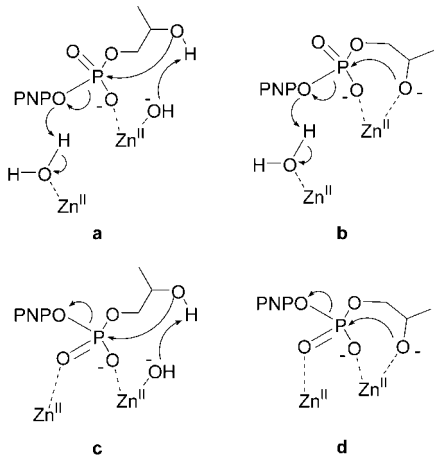

Figure 11. Proposed mechanisms for HPNP transesterification promoted by the Zn^{II} complexes of the peptides.

Conclusion

Several copies of the artificial amino acid ATANP have been efficiently inserted in proper positions in de novo designed polypeptides by using automated solid-phase synthesis. The new peptides (PRI–III) have been shown to adopt a well-defined tertiary structure characterized by a helix–loop–helix motif, which dimerizes in solution at concentrations above 200 μM to form a four-helix bundle. The above studies have also revealed that although the apopetides adopt the above conformation quite similarly to the parent systems used as reference in their design, the helical content is strongly dependent on pH and metal-ion binding. Both protonation of the amines of the triazacyclononane units present in the ATANP lateral arm and complexation with Zn^{II} ions cause a significant decrease of the helical content of the sequences. This appears to be at variance with what we have observed with oligopeptides incorporating C^{α}-tetrasubstituted amino acids as helix inducers that are extremely robust foldamers.[9b,d] It is likely that the conformational constraints introduced by α,α-disubstituted amino acids are such to support the charge repulsions and steric hindrance connected to the presence of the ATANP amino acid in a sequence.

Nevertheless the Zn^{II} complexes of the three peptides catalyze the transesterification of the RNA model substrate HPNP with different efficiency. The best catalyst appears to be PRI-4Zn^{II}, that is, the peptide incorporating four ATANP units. Michaelis–Menten saturation kinetics have allowed us to estimate that the substrate fully bound to the catalyst reacts 380 times faster than in its absence. The kinetic evidence suggests cooperativity between (at least two) metal ions with a mechanism requiring the activation of the nucleophilic species and its facilitated attack to the phosphate through its coordination to a Zn^{II} ion. Alternatively a Zn^{II}-bound water molecule may act as a general base. This latter possibility, however, seems less likely because of the pK_a of *p*-nitrophenol, the leaving group, which is lower than that of the Zn^{II}-bound H_2O.

The present systems constitute one of the few examples so far reported of synthetic peptides that act as efficient models of a multinuclear metallonuclease operating with a cooperative mechanism.[34]

Experimental Section

General: Solvents were purified by standard methods. All commercially available reagents and substrates were used as received. TLC analyses were performed using Merck 60 F_{254} precoated silica gel glass plates. Melting points were determined with a Büchi SMP-20 apparatus and are uncorrected. NMR spectra were recorded using a Bruker AM-250 (250 MHz) spectrometer. Chemical shifts are reported relative to internal Me_4Si (TMS). Multiplicity is given as usual. Optical rotations were determined on a Perkin–Elmer Model 241 polarimeter at 25 °C. ESI-MS spectra were obtained on a PE-API spectrometer at 5600 V by infusion of an MeOH/H_2O/acetic acid (10/90/1) mixture. $Cu(NO_3)_2$, $Zn(NO_3)_2$, and $ZnCl_2$ were analytical grade products. Metal-ion stock solutions were titrated against EDTA following standard procedures. The buffer components were used as supplied by the manufacturers: 4-(2-hydroxyethyl)-1-piperazineethanesulfonic acid (HEPES, Sigma), 2-(*N*-morpholino)ethanesulfonic acid (MES, Sigma) and 2-(*N*-cyclohexylamino)ethanesulfonic acid (CHES, Sigma).

(*N*-9-Fluorenylmethoxycarbonyl)-2-amino-3-{1-[1,4,7-(*N*-4-*N*-7-di-*tert*-butoxycarbonyl)triazacyclononane]}propanoic acid (Fmoc-ATANP-OH): Fmoc-ATANP-OH was obtained starting from (*N*-benzyloxycarbonyl)-2-amino-3-{1-[1,4,7-(*N*-4-*N*-7-di-*tert*-butoxycarbonyl)triazacyclononane]}-propanoic acid (Z-ATANP-OH).[11] Z-ATANP-OH (1.4 g, 2.54 mmol) was dissolved in methanol (10 mL) and the Z-protecting group was removed by hydrogenolysis with H_2 on Pd/C (5%). After filtration and evaporation of the solvent the deprotected amino acid H-ATANP-OH was obtained in quantitative yield. The amino acid was dissolved in water (20 mL) and *N*,*N*,*N*-triethylamine (TEA, 1.5 equivalents, 3.81 mmol) was added. A solution of 9-fluorenylmethyl-*N*-succinimidylcarbonate (Fmoc-OSu, 0.860 g, 2.56 mmol) in acetonitrile (5 mL) was added dropwise over a period of 10 minutes at room temperature. The reaction was followed, adjusting the pH to about 8 with TEA, and stirred overnight at room temperature. The solvent was evaporated under reduced pressure and the aqueous solution extracted once with diethyl ether (20 mL). The aqueous phase was acidified to pH 2–3 with $KHSO_4$ (10%) and extracted with ethyl acetate (3×50 mL). The organic phase was washed several times with water in order to eliminate *N*-hydroxysuccinimide (H-OSu) and dried over anhydrous Na_2SO_4; the solvent was evaporated. Pure Fmoc-ATANP-OH was obtained by precipitation from ethyl acetate/petroleum ether (1.22 g, 80% yield). $R_f = 0.6$ ($CHCl_3$/MeOH, 9/1); m.p. = 99–101 °C; $[\alpha]_D^{25} = +29.6$ ($c = 1$ in chloroform); ^{1}H NMR (250 MHz, $CDCl_3$, 25 °C, TMS): $\delta = 1.48$ (s, 18H; -$(CH_3)_3$), 3.49–3.08 (m, 14H; β-CH_2, -CH_2-CH_2-N), 4.22 (t, ^3J(H,H) = 6 Hz, 1H; CH Fmoc), 4.34 (m, 3H; -CH_2,OCO, -αCH), 6.01 (brs, 1H; NH), 7.36 (m, 4H; H2,2′, H3,3′ Fmoc), 7.59 (d, ^3J(H,H) = 7 Hz , 2H; H1,1′ Fmoc), 7.75 ppm (d, ^3J(H,H) = 7 Hz, 2H; H4,4′ Fmoc); ^{13}C NMR (63 MHz, $CDCl_3$, 25 °C, TMS): $\delta = 28.4$ (q), 47.1 (t), 48.6 (t), 50.3 (t), 54.3 (d), 55.4 (t), 59.0 (d) ,67.2 (t), 80.9 (s), 119.9 (d), 125.2 (d), 127.1 (d), 127.7 (d),141.2 (s), 143.8 (s),155.1 (s),155.6 (s), 156.3 (s), 172.7 (s).

PR I–III peptide syntheses: The peptides were synthesized by using a PerSeptive Biosystems Pioneer automated peptide synthesizer with a standard Fmoc chemistry protocol. The carboxy terminals were amidated upon cleavage from the resin using a Fmoc-PAL-PEG-PS polymer (PerSeptive Biosystems). The amino terminals were capped by acetic anhydride (0.3 mM in DMF). The peptides were cleaved from the polymer and deprotected with a mixture of trifluoroacetic acid (TFA, 13.5 mL), thioanisol (750 μL), 1,2-ethanedithiol (450 μL), and anisole (300 μL) at room temperature for 3 h. The crude peptides were precipitated by cold diethyl ether and collected by centrifugation. The peptides were purified by isochratic reversed phase HPLC on a C-8 semipreparative Kromasil (250 mm×2.5 mm), 7 μm column using different mixtures of isopropyl alcohol/water, 0.1% TFA, with a flow rate of 10 mL min^{-1} (PR I: 31% isopropyl alcohol; PR II–III: 35%). The peptides were eluted as single peaks and their purity was checked under identical conditions by reversed phase analytical HPLC. The peptides were identified by electrospray MS (PR I calculated 4660.515, found 4660.990; PR II calculated 4491.224, found 4490.850; PR III calculated 4491.224, found 4491.345) and the mass spectra obtained provided a further check of the purity of the peptides, since no other peaks were observed.

CD studies: CD spectra were recorded on a Jasco J-715 spectropolarimeter, routinely calibrated with (+)-camphor-10-sulphonic acid, in the wavelength interval 260–200 nm. Samples were prepared by diluting aqueous stock solutions, previously titrated by UV-visible spectroscopy with a standard solution of $Cu(NO_3)_2$ measuring the absorbance of the copper complex at 600 nm in 50 mM HEPES buffer at pH 7. The experiments were carried out in 0.1, 0.2, and 1 mm cells. The pH dependence was determined using proper buffers from pH 5–11 (pH 5–6, MES; 7–8, HEPES; 9–11, CHES) and the temperature-dependence experiments were peforemd with a water-jacked cell (0.1 mm) together with a circulating HAAKE constant temperature bath.

Kinetic measurements: Kinetic traces were recorded with a Unicam Helios β spectrophotometer equipped with a HAAKE temperature controller at 40 °C in 50 mM buffer (MES, HEPES, CHES). Fresh stock solutions of PR I–III and TACN were prepared in water (mQ) and the concentrations determined by UV-visible titration as described above. The PR I–4 Zn^{II}, PR II–2 Zn^{II}, PR III–2 Zn^{II}, and TACN–Zn^{II} complexes were prepared just before each experiment by dilution of the stock solutions through addition of proper aliquots of the buffer, water (mQ), and $Zn(NO_3)_2$ solutions up to a 0.8 mL final volume. The pH was checked before starting the measurement and the cuvettes were kept at 40 °C for 30 minutes before adding the substrate (HPNP). The reactions were carried out under turnover conditions using a tenfold excess of substrate over catalyst; the typical concentrations used were: [HPNP] = 2×10^{-4} M, [peptide] = 2×10^{-5} M.

The kinetics were followed at 400 nm (or 320 nm at a pH below 7), monitoring the release of 4-nitrophenolate (-phenol) up to a substrate conversion of 20%. The rate constants were obtained by using the method of initial rates. The absorbance versus time data of the first linear part of the reaction were converted into concentration versus time data by using the extinction coefficient for 4-nitrophenolate ($\varepsilon = 18700\ M^{-1}\,cm^{-1}$). Concentrations were corrected for the degree of ionization of the 4-nitrophenol at the operative pH. The slope of this initial linear part of the kinetic trace gives the initial rate (v_i, M s^{-1}) of the reaction. The second-order rate constants were obtained by dividing the initial rate by the analytical concentration of HPNP and peptide. In some experiments the reaction was followed to the total conversion of substrate. The kinetic traces registered followed a first-order process and the fitting of the data gave rate constants in good agreement with those obtained with the initial rate method.

Acknowledgments

P.S. and L.B. acknowledge partial support by the European Community's Human Potential Programme under contract HPRN-CT-1999–00008, ENDEVAN. Support by the Ministry of Education, University, and Research of Italy (MIUR, contract 2002031238) to P.S. and P.T. is also gratefully acknowledged.

[1] N. Voyer, J. Lamothe, *Tetrahedron* **1995**, *51*, 9241–9284.
[2] S. M. Gellman, *Acc. Chem. Res.* **1998**, *31*, 173–180.
[3] N. H. William, P. Wyman, *Chem. Commun.* **2001**, 1268–1269.
[4] a) D. E. Wilcox, *Chem. Rev.* **1996**, *96*, 2435–2458; b) N. Sträter, W. N. Lipscomb, T. Klabunde, B. Krebs, *Angew. Chem.* **1996**, *108*, 2158–2191; *Angew. Chem. Int. Ed. Engl.* **1996**, *35*, 2024–2055.
[5] M. D. Sam, J. J. Perona, *Biochemistry* **1999**, *38*, 6576–6586.
[6] a) N. H. Williams, B. Takasaki, M. Wall, J. Chin, *Acc. Chem. Res.* **1999**, *32*, 485–493; b) E. L. Hegg, J. N. Burstyn, *Coord. Chem. Rev.* **1998**, *173*, 133–165.
[7] a) P. Molenveld, J. F. J. Engbersen, D. N. Reinhoudt, *Angew. Chem.* **1999**, *111*, 3387–3390; *Angew. Chem. Int. Ed.* **1999**, *38*, 3189–3191; b) M. J. Young, J. Chin, *J. Am. Chem. Soc.* **1995**, *117*, 10577–10578; c) K. O. A. Chin, J. R. Morrow, *Inorg. Chem.* **1994**, *33*, 5036–5041; d) S. Liu, Z. Luo, A. D. Hamilton, *Angew. Chem.* **1997**, *109*, 2794–2796; *Angew. Chem. Int. Ed. Engl.* **1997**, *36*, 2678–2680; e) M. Irisawa, N. Takeda, M. Komijama, *J. Chem. Soc. Chem. Commun.* **1995**, 1221–1222; f) B. Linkletter, J. Chin, *Angew. Chem.* **1995**, *107*, 529;

Angew. Chem. Int. Ed. Engl. **1995**, *34*, 472–474; g) W. H. Chapman Jr. , R. Breslow, *J. Am. Chem. Soc.* **1995**, *117*, 5462–5469.
[8] a) K. G. Ragunhatan, H.-J. Schneider, *Angew. Chem.* **1996**, *108*, 1314–1316; *Angew. Chem. Int. Ed. Engl.* **1996**, *35*, 1219–1221; b) H.-J. Schneider, R. Hettich, *J. Am. Chem. Soc.* **1997**, *119*, 5638–5647.
[9] a) P. Rossi, F. Felluga, P. Tecilla, F. Formaggio, M. Crisma, C. Toniolo, P. Scrimin, *J. Am. Chem. Soc.* **1999**, *121*, 6948–6949; b) P. Rossi, F. Felluga, P. Tecilla, F. Formaggio, M. Crisma, C. Toniolo, P. Scrimin, *Biopolymers, Pept. Sci.* **2000**, *55*, 496–501; c) C. Sissi, P. Rossi, F. Felluga, F. Formaggio, M. Palumbo, P. Tecilla, C. Toniolo, P. Scrimin, *J. Am. Chem. Soc.* **2001**, *123*, 3169–3170; d) A. Scarso, U. Scheffer, M. Göbel, Q. B. Broxterman, B. Kaptein, F. Formaggio, C. Toniolo, P. Scrimin, *Proc. Natl. Acad. Sci. USA* **2002**, *99*, 5144–5149.
[10] P. Pengo, L. Pasquato, S. Moro, A. Brigo, F. Fogolari, Q. B. Broxterman, B. Kaptein, P. Scrimin, *Angew. Chem.* **2003**, *115*, *3510–3514; Angew. Chem. Int. Ed.* **2003**, *42*, 3388–3392.
[11] P. Rossi, F. Felluga, P. Scrimin, *Tetrahedron Lett.* **1998**, *39*, 7159–7162.
[12] L. Baltzer, K. S. Broo, *Biopolymers* **1998**, *47*, 31–40.
[13] G. T. Dolphin, L. Brive, G. Johansson, L. Baltzer, *J. Am. Chem. Soc.* **1996**, *118*, 11297–11298.
[14] L. Brive, G. T. Dolphin, L. Baltzer, *J. Am. Chem. Soc.* **1997**, *119*, 8598–8607.
[15] R. B. Hill, W. F. De Grado, *J. Am. Chem. Soc.* **1998**, *120*, 1138–1145.
[16] S. F. Betz, W. F. De Grado, *Biochemistry*, **1996**, *35*, 6955–6962.
[17] M. D. Struthers, R. P. Cheng, B. Imperiali, *Science*, **1996**, *271*, 342–325.
[18] S. K. Broo, L. Brive, P. Ahlberg, L. Baltzer, *J. Am. Chem. Soc.* **1997**, *119*, 11362–11372.
[19] a) S. Olofsson, G. Johansson, L. Baltzer, *J. Chem. Soc. Perkin Trans. 2* **1995**, 2047–2056; b) J. Nilsson, K. S. Broo, R. S. Sott, L. Baltzer, *Can. J. Chem.* **1999**, *77*, 990–996; c) J. Nilsson, L. Baltzer, *Chem. Eur. J.* **2000**, *6*, 2214–2220.
[20] S. Olofsson, L. Baltzer, *Folding Des.* **1996**, *1*, 347–356.
[21] Y. H. Chen, J. T. Yang, K. H. Chan, *Biochemistry* **1974**, *13*, 3350–3359.
[22] M. Engel, R. W. Williams, B. W. Erickson, *Biochemistry* **1991**, *30*, 3161–3169.
[23] R. M. Smith, A. E. Martell, *Critical Stability Constants*, *Vol. 6* Plenum, New York, **1989**.
[24] L. Baltzer, H. Nilsson, J. Nilsson, *Chem. Rev.* **2001**, *101*, 3153–3164.
[25] N. Greenfield, G. D. Fasman, *Biochemistry* **1969**, *8*, 4108–4116.
[26] "Mechanisms in Protein Folding": *Frontiers in Molecular Biology* (Ed.: R. H. Pain), Oxford University Press, Oxford, **1994**.
[27] A reviewer pointed out the discrepancy between the Cu^{II} and Zn^{II} binding experiments as it appears that Zn^{II} binds more strongly than Cu^{II} contrary to expectations (the plateaux is reached at ca. four equivalents of added ions). We believe that the apparent levelling off of the ellipticity is the result of two opposite effects due to metal ion binding: a higher lipophilicity of the peptide related to deprotonation (helical content increases, see Figure 3) and electrostatic repulsion (helical content decreases). Likely in that concentration range the two effects are very similar.
[28] S. Y. M. Lau, A. K. Taneja, R. S. Hodges, *J. Biol. Chem.* **1984**, *259*, 13253–13261.
[29] Because the metal complexes used in the kinetic experiments are formed in situ and the experiments show that there is not complete binding of the Zn^{II} ions to the peptides, throughout the paper we use the notation PR(I–III)–*n*Zn^{II} to indicate these complexes. This does not imply that we are dealing with the *n* nuclear complexes. In fact, as clearly shown for PR I, the real molecularity of the complexes is not known and in most cases is less than *n*.
[30] The pseudo-first-order rate constant for the uncatalyzed cleavage of HPNP at pH 7.4 and 313 K is $4.0\times10^{-7}\,s^{-1}$. This corresponds to an initial rate of cleavage (v_i) of $8.0\times10^{-11}\,M\,s^{-1}$ for a $2.0\times10^{-4}\,M$ concentration of substrate.
[31] a) K. Michaelis, M. Kalesse, *Angew. Chem.* **1999**, *111*, 2382–2385; *Angew. Chem. Int. Ed.* **1999**, *38*, 2243–2245; b) J. C. Verheijen, B. Deiman, E. Y. Yeheskiely, G. A. van der Marel, J. H. Van Boom, *Angew. Chem.* **2000**, *112*, 377–380; *Angew. Chem. Int. Ed.* **2000**, *39*, 369–372.
[32] K. Worm, F. Chu, K. Matsumoto, M. D. Best, V. Lynch, E. V. Anslyn, *Chem. Eur. J.* **2003**, *9*, 741–747.
[33] P. Molenveld, W. M. G. Stickvoort, H. Kooijman, A. L. Spek, J. F. J. Engbersen, D. N. Reinhoudt, *J. Org. Chem.* **1999**, *64*, 3896–3906.
[34] A. Scarso, P. Scrimin in *Pseudo-Peptides in Drug Development* (Ed.: P. E. Nielsen), Wiley-VCH, Weinheim, **2004**, pp. 223–240.

Received: February 18, 2004
Published online: July 14, 2004

